Calcium Binding Properties of the *Kingella kingae* PilC1 and PilC2 Proteins Have Differential Effects on Type IV Pilus-Mediated Adherence and Twitching Motility

Eric A. Porsch,[a,b] Michael D. L. Johnson,[c*] Angela D. Broadnax,[d] Christopher K. Garrett,[c,d] Matthew R. Redinbo,[c,d,e] Joseph W. St. Geme III[a,b]

Department of Pediatrics[a] and Department of Molecular Genetics and Microbiology,[b] Duke University Medical Center, Durham, North Carolina, USA; Department of Biochemistry and Biophysics,[c] Department of Chemistry,[d] and Department of Microbiology and Immunology,[e] University of North Carolina at Chapel Hill, Chapel Hill, North Carolina, USA

Kingella kingae **is an emerging bacterial pathogen that is being recognized increasingly as an important etiology of septic arthritis, osteomyelitis, and bacteremia, especially in young children. The pathogenesis of *K. kingae* disease begins with bacterial adherence to respiratory epithelium, which is dependent on type IV pili and is influenced by two PilC-like proteins called PilC1 and PilC2. Production of either PilC1 or PilC2 is necessary for *K. kingae* piliation and bacterial adherence. In this study, we set out to further investigate the role of PilC1 and PilC2 in type IV pilus-associated phenotypes. We found that PilC1 contains a functional 9-amino-acid calcium-binding (Ca-binding) site with homology to the *Pseudomonas aeruginosa* PilY1 Ca-binding site and that PilC2 contains a functional 12-amino-acid Ca-binding site with homology to the human calmodulin Ca-binding site. Using targeted mutagenesis to disrupt the Ca-binding sites, we demonstrated that the PilC1 and PilC2 Ca-binding sites are dispensable for piliation. Interestingly, we showed that the PilC1 site is necessary for twitching motility and adherence to Chang epithelial cells, while the PilC2 site has only a minor influence on twitching motility and no influence on adherence. These findings establish key differences in PilC1 and PilC2 function in *K. kingae* and provide insights into the biology of the PilC-like family of proteins.**

*K*ingella kingae is a Gram-negative organism that belongs to the Neisseriaceae family and is being recognized increasingly as an important pathogen in young children. Improvements in culture-based and molecular diagnostics have identified *K. kingae* as a common etiology of septic arthritis, osteomyelitis, and bacteremia in the pediatric population (1–8). A recent study reported *K. kingae* as the leading cause of septic arthritis in children 6 to 36 months of age (1). Based on epidemiological studies, *K. kingae* is believed to initiate infection by colonizing the posterior pharynx, where it typically persists for weeks without producing symptoms (9–12). On occasion, the organism will breach the epithelial barrier and enter the bloodstream and then disseminate hematogenously to the joints, bones, or endocardium (6, 8). This model is supported by reports describing genotypically identical *K. kingae* paired isolates from the respiratory tract and blood of patients with invasive *K. kingae* disease (11, 13). Despite increased recognition of *K. kingae* as an important pathogen, little is known about the molecular mechanisms used by this organism to cause disease.

Previous work established that *K. kingae* produces type IV pili that are necessary for adherence to respiratory epithelial and synovial cells (14–16). Type IV pili are surface fibers that are widespread in Gram-negative bacteria and convey many phenotypes, including adherence, twitching motility, and natural competence (17, 18). These fibers are composed primarily of a single protein subunit (called PilA1 in *K. kingae*) and require numerous other factors for proper production. A key aspect of type IV pilus biology and the associated phenotypes is the ability of the fiber to be retracted through the outer membrane, a process catalyzed by the retraction ATPase, PilT, and associated with twitching motility (19–23). While many of the protein factors involved in type IV pilus biology have been well studied, the mechanism controlling

pilus extension and pilus retraction remains poorly understood. However, current data from work on the pathogenic *Neisseria* species (*Neisseria meningitidis* and *Neisseria gonorrhoeae*) and *Pseudomonas aeruginosa* suggests that counteraction of retraction by PilC-like proteins is required for proper pilus production and twitching motility (24–26).

The PilC proteins are proposed to influence two aspects of type IV pilus biology, namely, pilus biogenesis and adherence. Like *N. meningitidis* and *N. gonorrhoeae*, *K. kingae* produces two PilC-like proteins called PilC1 and PilC2, which are encoded by genes at separate locations in the genome (14, 27, 28). The PilC1 and PilC2 proteins in the pathogenic *Neisseria* species have been identified as the adhesive component of the pilus fiber and are located at the tip of the fiber in *N. gonorrhoeae* (29–31). Recent observations suggest that *P. aeruginosa* PilY1 (the single PilC-like protein in *P. aeruginosa*) is also an adhesin (25, 32). In earlier work, we observed a reduction in adherence to human cells by *K. kingae* strain 269-492 derivatives that expressed only PilC1 or PilC2, supporting a po-

doi:10.1128/JB.02186-12

tential role for these proteins in adherence (14). In addition, we found that elimination of both PilC1 and PilC2 in *K. kingae* strain 269-492 resulted in a loss of piliation, suggesting that at least one PilC protein is required for pilus production (14). Similar results were obtained with the pathogenic *Neisseria* species and *P. aeruginosa* (27, 33). Recently, *P. aeruginosa* PilY1 was shown to regulate pilus production and twitching motility through calcium binding (Ca binding) at a 9-amino-acid loop in the C-terminal domain (34). Using bioinformatic approaches, similar loops were identified in other PilC homologs, including *N. meningitidis* and *N. gonorrhoeae* PilC1 and PilC2 and *K. kingae* PilC1, but not PilC2 (34).

In contrast to the PilC1 and PilC2 proteins in *N. gonorrhoeae* and *N. meningitidis*, *K. kingae* PilC1 and PilC2 share only limited overall sequence homology (7% identity and 16% similarity) (14). In this regard, *K. kingae* represents a unique and intriguing system to investigate PilC-like protein biology. In this study, we examined Ca binding by PilC1 and PilC2 and the potential role of Ca binding in control of type IV pilus production, twitching motility, and adherence to Chang epithelial cells. We report that both PilC1 and PilC2 bind calcium, with PilC1 utilizing a 9-amino-acid PilY1-like Ca-binding site and PilC2 utilizing a 12-amino-acid human calmodulin-like Ca-binding site. While both the PilC1 and PilC2 Ca-binding sites are dispensable for pilus production, the PilC1 Ca-binding site is required for twitching motility and adherence.

MATERIALS AND METHODS

Bacterial strains. Bacterial strains used in this study are listed in Table 1. *K. kingae* strains were stored at −80°C in brain heart infusion broth (BHI) with 30% glycerol. *K. kingae* strain KK03 is a stable high-level pilus-expressing, spreading-corroding colony type (bacterial growth spreads from the central raised colony, and colony expansion results in pitting or corroding of the agar surface) of clinical isolate 269-492. *E. coli* strains were stored at −80°C in Luria-Bertani (LB) broth with 15% glycerol. *K. kingae* strains were routinely cultured at 37°C with 5% CO_2 on chocolate agar supplemented with 50 μg/ml kanamycin, 1 μg/ml erythromycin, or 2 μg/ml tetracycline, as appropriate. *E. coli* strains were routinely cultured at 37°C in LB broth or on LB agar supplemented with 100 μg/ml ampicillin, 50 μg/ml kanamycin, 500 μg/ml erythromycin, 25 μg/ml tetracycline, 50 μg/ml streptomycin, or 50 μg/ml chloramphenicol, as appropriate.

Recombinant PilC constructs and protein purification. All plasmids used in this study are listed in Table 1, and all primers are listed in Table S1 in the supplemental material. PilC1 residues 739 to 1047 were cloned from pUC19*pilC1* with primers PilC1 738 F and PilC1 1047 R into a pMCSG9 LIC HIS MBP vector. Site-directed mutagenesis was performed to produce D930A and D930K mutations with primers PilC1D930A-F/PilC1D930A-R and PilC1D930K-F/PilC1D930K-R, respectively. All clones were confirmed by nucleotide sequencing. Resultant vectors were transformed into BL21-RIPL cells (Stratagene) and plated on LB agar plates containing 25 μg/ml tetracycline, 50 μg/ml streptomycin, 50 μg/ml chloramphenicol, and 100 μg/ml ampicillin. A single colony was used to inoculate 50 ml of LB broth containing the previously mentioned antibiotics, and cultures were incubated overnight. Cell cultures were centrifuged at 3,000 × *g*, and the supernatant was discarded. The resultant pellet was used to inoculate a 1.5-liter shaker flask of Terrific broth (TB) with 50 μl antifoam (Sigma-Aldrich) and the previously mentioned antibiotics. Cells were grown at 37°C until the optical density at 600 nm (OD_{600}) reached 0.6 to 0.8. The temperature was then reduced to 18°C, and protein expression was induced with 0.2 mM isopropyl-β-D-thiogalactopyranoside (IPTG). Cells were grown overnight and harvested by centrifugation at 6,000 × *g* at for 15 min at 4°C, and pellets were stored at −80°C.

Thawed PilC1 pellets were suspended in lysis buffer (50 mM sodium phosphate [pH 7.6], 500 mM NaCl, 25 mM imidazole) supplemented with 0.5 mM EDTA, 0.1% Triton X-100, 1 mM phenylmethylsulfonyl fluoride (PMSF), one tablet of a protease inhibitor cocktail (Roche), and 1 μg/ml lysozyme. After 1 h of gentle stirring on ice, the cells were sonicated on ice for 1 min and the lysate was centrifuged at 45,000 × *g* for 90 min at 4°C. Using an ÄKTAxpress (GE Healthcare), protein from the filtered soluble fraction was nickel purified (elution buffer consisted of 50 mM sodium phosphate [pH 7.6], 500 mM NaCl, and 500 mM imidazole) and purified on an S200 gel filtration column in the final buffer, which contained 20 mM Tris-HCl (pH 7.5), 250 mM NaCl, 2 mM dithiothreitol (DTT), and 5% glycerol. Protein was then concentrated, flash frozen in liquid nitrogen, and stored at −80°C.

PilC2 residues 868 to 1502 were cloned from genomic *K. kingae* DNA with primers PilC2 868 F and PilC2 end R into a pMCSG7 LIC HIS vector. Site-directed mutagenesis was performed to produce D1125A (primers PilC2D1125A-F/PilC2D1125A-R), D1125K (primers PilC2D1125K-F/PilC2D1125K-R), D1444A (primers PilC2D1444A-F/PilC2D1444A-R), and D1444K (primers PilC2D1444K-F/PilC2D1444K-R) mutations. Resultant plasmids were transformed into BL21-Gold cells (Agilent), which were incubated overnight on LB plates containing ampicillin. Subsequently, a single colony was used to inoculate 100 ml LB broth overnight containing 50 μg/ml ampicillin, and the culture was incubated overnight. Cell cultures were treated as described above except that they were induced with 0.5 mM IPTG.

Cells pellets were thawed and resuspended in buffer consisting of 10 mM Tris (pH 7.8) and 50 mM NaCl with 10 mM imidazole, DNase, and protease inhibitor tablets (Roche). Cells were sonicated, and the cell lysate was separated into soluble and insoluble fractions using high-speed centrifugation. The soluble fraction was filtered, then nickel purified (with 300 mM imidazole), buffer exchanged (no imidazole), and separated using an S200 gel filtration column on an ÄKTAxpress (GE Healthcare). If necessary, protein and storage buffers were chelated with Chelex-100 to remove bound calcium (Bio-Rad Laboratories). Purified proteins were concentrated to ~100 μM, frozen, and stored at −80°C.

***K. kingae* strain construction.** Gene disruptions and directed mutations were generated in *K. kingae* as previously described (14, 15). Briefly, plasmid-based disruption constructs were created in *E. coli*, linearized, and introduced into *K. kingae* strain KK03 via natural transformation and plating on appropriate antibiotic-containing media. Correct localization of disruptions was confirmed by PCR or Southern blotting, and site-directed mutations were confirmed by nucleotide sequencing. The Δ*pilF* and Δ*pilC1* deletion constructs were generated as previously described (14). As our original *pilC2* disruption was an insertional transposon mutant (14), we decided to generate a targeted Δ*pilC2* deletion. PCR fragments corresponding to the 5′ and 3′ regions of *pilC2* were amplified individually from strain KK03 with primers *pilC2*Δ5′F/*pilC2*Δ5′R and *pilC2*Δ3′F/*pilC2*D3′R and were then ligated into EcoRI/HindIII-digested pUC19, generating pUC19*pilC2*::BamHI, which contains a large *pilC2* internal deletion and a BamHI site. The kanamycin resistance cassette *aphA3* was PCR amplified with primers *aphA3*FBamHI/*aphA3*RBamHI from pFalcon2 and ligated into BamHI-digested pUC19*pilC2*::BamHI, generating pUC19Δ*pilC2*.

To generate *pilC* alleles that encode Ca-binding site mutations, antibiotic resistance markers were inserted adjacent to the *pilC* gene in a pUC19 backbone, subjected to site-directed mutagenesis, sequenced, linearized, and transformed into *K. kingae* strain KK03. For PilC1 Ca-binding site mutations, the entire *pilC1* gene and ~1,000 bp of 5′ and 3′ flanking sequence were PCR amplified from KK03 genomic DNA with primers *pilC1*regionF/*pilC1*regionR and the ligated into EcoRI/SalI-digested pUC19, generating pUC19*pilC1*. The QuikChange XL-II site-directed mutagenesis kit (Agilent) and primers *pilC1*markF/*pilC1*markR were used to insert an MluI site in the gene upstream of the *pilC1* promoter region, a predicted ABC-type transporter, generating pUC19/MluI*pilC1*. The *ermC* erythromycin resistance cassette was amplified from pIDN4 with primers *ermC*F/*ermC*R and was ligated into MluI-di-

TABLE 1 Strains and plasmids used in this study

Strain or plasmid	Description	Reference or source
E. coli strains		
Dh5α	*E. coli* F⁻ ϕ80d*lacZ*ΔM15 Δ(*lacZYA-argF*)U169 *deoR recA1 endA1 hsdR17*(r$_K^-$ m$_K^+$) *phoA supE441 thi-1 gyrA96 relA1*	49
BL21-CodonPlus(DE3)-RIPL	*E. coli* B F⁻ *ompT hsdS*(r$_B^-$ m$_B^-$) *dcm*⁺ Tetr *gal* λ(DE3) *endA* Hte [*argU proL*Camr] [*argU ileY leuW* Strep/Specʳ]	Agilent
BL21-Gold(DE3)	*E. coli* B F⁻ *ompT hsdS*(r$_B^-$ m$_B^-$) *dcm*⁺ Tetʳ *gal* λ(DE3) *endA* Hte	Agilent
K. kingae strains		
KK03	Naturally occurring spreading and corroding variant of septic arthritis clinical isolate 269-492	36
KK03 derivatives (genotype or phenotype)		
Δ*pilF*	KK03 with an *aphA3* marked *pilF* deletion	This work
Δ*pilT*	KK03 with an *ermC* marked *pilT* insertion	38
Δ*pilC1*	KK03 with a *tetM* marked *pilC1* deletion	This work
Δ*pilC2*	KK03 with an *aphA3* marked *pilC2* deletion	This work
Δ*pilC1* Δ*pilC2*	KK03 with a *tetM* marked *pilC1* deletion and an *aphA3* marked *pilC2* deletion	This work
Δ*pilC1* PilC2mark	*pilC1*-bearing strain with an *aphA3* insertion immediately downstream of WT *pilC2*	This work
Δ*pilC2* PilC1mark	*pilC2*-bearing strain with an *ermC* insertion upstream of WT *pilC1*	This work
Δ*pilC1* PilC2D1444A	Δ*pilC1* PilC2mark strain with a *pilC2* mutation resulting in expression of PilC2D1444A	This work
Δ*pilC1* PilC2D1444K	Δ*pilC1* PilC2mark strain with a *pilC2* mutation resulting in expression of PilC2D1444K	This work
Δ*pilC2* PilC1D930A	Δ*pilC2* PilC1 mark strain with a *pilC1* mutation resulting in expression of PilC1D930A	This work
Δ*pilC2* PilC1D930K	Δ*pilC2* PilC1 mark strain with a *pilC1* mutation resulting in expression of PilC1D930K	This work
PilC1D930A PilC2D1444A	Strain KK03 expressing PilC1D930A and PilC2D1444A	This work
PilC1D930K PilC2D1444K	Strain KK03 expressing PilC1D930K and PilC2D1444K	This work
Plasmids		
pMCSG7	Protein expression vector for 6× His N-terminal fusions and a TEV cleavage site	50
pMCSG9	Protein expression vector for MBP 6× His N-terminal fusions and a TEV cleavage site	51
pMCSG9/PilC1	For expression of MBP-PilC1$_{739-1047}$	This work
pMCSG9/PilC1D930A	For expression of MBP-PilC1$_{739-1047}$ D930A	This work
pMCSG9/PilC1D930K	For expression of MBP-PilC1$_{739-1047}$ D930K	This work
pMCSG7/PilC2	For expression of HIS-PilC2$_{868-1502}$	This work
pMCSG7/PilC2D1125A	For expression of HIS-PilC2$_{868-1502}$ D1125A	This work
pMCSG7/PilC2D1125K	For expression of HIS-PilC2$_{868-1502}$ D1125K	This work
pMCSG7/PilC2D1444A	For expression of HIS-PilC2$_{868-1502}$ D1444A	This work
pMCSG7/PilC2D1444K	For expression of HIS-PilC2$_{868-1502}$ D1444K	This work
pFalcon2	Source of *aphA3* kanamycin resistance gene	52
pHSX*tetM*4	Source of *tetM* tetracycline resistance gene	53
pIDN4	Source of *ermC* erythromycin resistance gene	54
pUC19/Δ*pilF*	*pilF* deletion construct	36
pUC19/Δ*pilC1*	*pilC1* deletion construct	14
pUC19/Δ*pilC2*	*pilC2* deletion construct	This work
pUC19/Erm*pilC1*	For introduction of *ermC* marked *pilC1* locus	This work
pUC19/*pilC2*Kan	For introduction of *aphA3* marked *pilC2* locus	This work
pUC19/PilC1D930A	For introduction of PilC1D930A	This work
pUC19/PilC1D930K	For introduction of PilC1D930K	This work
pUC19/PilC2D1444A	For introduction of PilC2D1444A	This work
pUC19/PilC2D1444K	For introduction of PilC2D1444K	This work

gested pUC19/MluI*pilC1*, generating pUC19/Erm*pilC1*. Restriction digestion and sequencing were used to confirm proper orientation of *ermC*. To confirm that the *ermC* marker inserted upstream of WT *pilC1* did not alter the phenotypes observed in the Δ*pilC2* background, a control Δ*pilC2*/PilC1mark (*pilC2* deleted and *ermC* upstream of *pilC1*) strain was created and was confirmed to have phenotypes identical to those of the Δ*pilC2* strain. Site-directed mutagenesis with primers PilC1D930A-F/

PilC1D930A-R and PilC1D930K-F/PilC1D930K-R was used to generate the D930A and D930K mutations, respectively.

For the PilC2 Ca-binding site mutations, ~2.6 kb of the 3′ region of *pilC2* was amplified with primers *pilC2*markAF/*pilC2*markAR and ~1.5 kb of sequence immediately downstream of the *pilC2* open reading frame (ORF) was amplified with primers *pilC2*markBF/*pilC2*markBR individually from KK03 genomic DNA and ligated into EcoRI/HindIII-digested

pUC19, generating pUC19*pilC2*, which contains a BamHI site inserted 20 bp downstream of the *pilC2* stop codon. The kanamycin resistance cassette *aphA3* was PCR amplified with primers *aphA3*FBamHI/*aphA3*RBamHI from pFalcon2 and ligated into BamHI-digested pUC19*pilC2*, generating pUC19*pilC2*Kan. To confirm that the *aphA3* marker inserted immediately downstream of wild-type (WT) *pilC2* did not alter the phenotypes observed in the *K. kingae* Δ*pilC1* background, a control Δ*pilC1* PilC2mark (*pilC1* deleted and *aphA3* inserted downstream of *pilC2*) strain was created and confirmed to have phenotypes identical to those of the Δ*pilC1* strain. Site-directed mutagenesis with primers PilC2D1444A-F/PilC2D1444A-R and PilC2D1444K-F/PilC2D1444K-R was used to generate the D1444A and D1444K mutations, respectively.

Calcium binding assay. A binding curve for Oregon green 488 BAPTA-5N, hexapotassium salt (Invitrogen) in 10 mM Tris (pH 7.8) and 50 mM NaCl was measured on a PHERAstar (BMGLabtech) at 488 nm. Purified PilC1 or PilC2 was chelated with Chelex-100 resin (Bio-Rad) and subsequently serially diluted 1.5- to 3-fold from ~100 μM to ~1 nM, and each dilution was combined with 20 μM Oregon green and 2 μM CaCl$_2$ and measured at 488 nm on a PHERAstar (BMGLabtech) to obtain a 50% effective concentration (EC$_{50}$). The EC$_{50}$ was then used to calculate the respective K_d (dissociation constant) for calcium as described previously (34).

CD and thermal denaturation. Protein samples were exchanged into chelated 10 mM K$_x$H$_x$PO$_4$–50 mM NaF (pH 7.7) buffer, where x is dependent on pH, and brought to 5 μM with or without the addition of 20 μM CaCl$_2$. A wavelength scan from 200 to 260 nm was performed on a circular-dichroism (CD) spectrometer 62 DS (Aviv) at 16°C with a 10-s averaging time. Melting temperatures were measured at 214 nm from 3°C to 95°C at 1-degree increments with a 10-s averaging time.

Pilus preparations. Derivatives of *K. kingae* strain KK03 were incubated on chocolate agar for 17 to 18 h, and growth was suspended in 1.5 ml 50 mM Tris–150 mM NaCl (pH 8.0) to an OD$_{600}$ of 1.0, vortexed at full speed for 1 min, and centrifuged at 21,000 × *g* for 2 min to pellet the bacteria. A total of 1.25 ml of the bacterium-free supernatant was subjected to 20% ammonium sulfate precipitation on ice for 2 h. Precipitated pili were collected via centrifugation at 21,000 × *g* for 5 min and resuspended in 1× SDS-PAGE loading buffer. Aliquots were separated on 15% SDS-PAGE gels and stained with Coomassie blue. The observed protein band was confirmed to be the major pilin subunit, PilA1, by Western blotting with antiserum GP65 as described previously (15).

Twitching-motility assays. Twitching motility was assessed by a modified agar plate stab assay originally developed for *P. aeruginosa* (35). Briefly, derivatives of *K. kingae* strain KK03 were incubated on chocolate agar for 17 to 18 h, and growth was resuspended in 1× phosphate-buffered saline (PBS) to an OD$_{600}$ of 1.0. One microliter of the bacterial suspension was stab inoculated to the bottoms of tissue culture-treated 100-mm plates containing 10 ml chocolate agar with 1% agar and incubated at 37°C with 5% CO$_2$ for 48 h. To reduce zone-to-zone and plate-to-plate variation, the twitching-motility plates were cooled at ambient temperature for 24 h prior to stab inoculation, and each strain set replicate was performed with the same batch of chocolate agar plates. Twitching-motility-competent strains spread from the stab inoculation site at the plate-agar interface. The agar was carefully peeled away, and the plate was air dried and stained with crystal violet to visualize the twitching-motility zones. Three diameter measurements were taken and averaged per twitching zone. All experiments were performed in triplicate, and error bars represent standard errors of the means. Statistical analysis was performed using analysis of variance (ANOVA) and Bonferroni's posttest to compare twitching zones between mutant and parental strains.

Eukaryotic cell lines. Chang cells (Wong-Kilbourne derivative [D] of Chang conjunctiva, HeLa origin; ATCC CCL-20.2) were cultivated at 37°C with 5% CO$_2$ in media as described previously (36).

Adherence assays. Quantitative adherence assays were performed as described previously (14, 15). Briefly, monolayers of fixed Chang cells at a density of ~2 × 10^5/well in 24-well plates were inoculated with approxi-

mately 6.5 × 10^6 CFU of bacteria (multiplicity of infection [MOI] of ~30), and plates were centrifuged at 165 × *g* for 5 min and then incubated for 25 min at 37°C in 5% CO$_2$. Monolayers were washed 4 times with PBS to remove nonadherent bacteria and were then treated with 1× trypsin-EDTA (Sigma) for 20 min at 37°C to release adherent bacteria. Appropriate dilutions were plated on chocolate agar, and percent adherence was calculated by dividing the number of adherent CFU by the number of inoculated CFU. All experiments were performed in triplicate. Statistical analysis was performed using ANOVA and Bonferroni's posttest to compare adherence levels between mutant and parental strains.

Transmission electron microscopy (TEM). To assess surface piliation, *K. kingae* strains were resuspended in ammonium acetate, pH 7.4, and allowed to absorb onto Formvar-carbon-coated 200-mesh grids for 1 min. The grids were subsequently stained with 1% uranyl acetate for 30 s, excess liquid was wicked away, and the grids were air dried and examined on a Philips CM12 transmission electron microscope (TEI) at an accelerating voltage of 80 kV.

RESULTS

K. kingae **PilC1 and PilC2 contain a calcium-binding site.** Based on sequence homology with *P. aeruginosa* PilY1 and *N. meningitidis* and *N. gonorrhoeae* PilC1 and PilC2, *K. kingae* encodes two PilC homologs called PilC1 and PilC2. Interestingly, while PilC1 and PilC2 in the pathogenic *Neisseria* species are nearly identical, the *K. kingae* strain 269-492 PilC1 and PilC2 proteins share only limited homology with each other and with other PilC-like protein family members (14). Most of the similarity between members of this protein class resides in the C-terminal putative pilus-interacting half of the proteins (34). Interestingly, while *K. kingae* is a member of the *Neisseriaceae* family, the PilC1 and PilC2 C-terminal domains are more similar to *P. aeruginosa* PilY1 than to the *Neisseria* PilC1 and PilC2 proteins or even to each other (Fig. 1A and C). The difference in length of PilC1 and PilC2 compared to *P. aeruginosa* PilY1 reflects the presence of multiple nonhomologous sequences in PilC1 and PilC2 that are absent in PilY1. Examination of the *K. kingae* PilC1 and PilC2 amino acid sequences revealed one predicted Ca-binding site in each protein (Fig. 1B and D). PilC1 contains a 9-residue site (922-DVNRDGVYD-930) that is similar to the Ca-binding loop in *P. aeruginosa* PilY1 (Fig. 1B), and PilC2 contains a 12-residue site (1433-DTNGDGKFTEAD-1444) with strong homology to the canonical EF-hand human calmodulin Ca-binding loop (Fig. 1D). An additional less conserved 12-residue calmodulin-like Ca-binding site was also identified in PilC2 (1114-DLTNPTDLTESD-1125) (Fig. 1D).

To determine if the putative PilC1 Ca-binding site binds calcium, recombinant fragments of PilC1 were expressed in *E. coli*, purified, and tested for Ca-binding potential *in vitro*. A C-terminal PilC1 fragment containing amino acids 739 to 1047 was expressed as a maltose-binding protein (MBP) fusion, PilC1$_{739-1047}$-MBP, and purified. As shown in Fig. 2A, PilC1$_{739-1047}$-MBP exhibited a binding affinity for calcium with a K_d of 530 nM, confirming that PilC1 binds calcium. The affinity of PilC1 is comparable to the affinity of PilY1, which has a K_d of 2.6 μM (34). Orans et al. demonstrated that mutation of the terminal bidentate aspartic acid residue in the PilY1 9-amino-acid Ca-binding loop to alanine eliminated Ca binding and created a calcium-free PilY1 state, while mutation of this residue to lysine also eliminated Ca binding but created a potential calcium-bound mimic PilY1 state (34). As shown in Fig. 2A, mutation of the terminal aspartic acid residue D930 in the *K. kingae* PilC1 Ca-binding site to either alanine or lysine eliminated specific Ca binding. The mutant
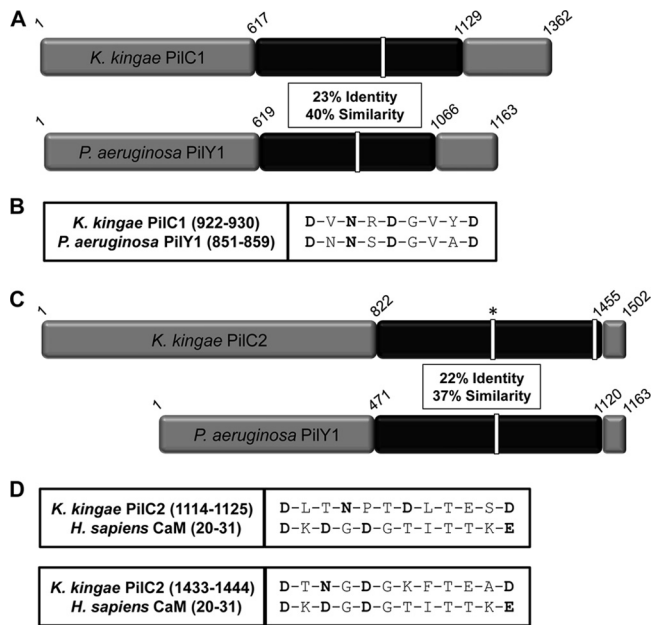
FIG 1 (A) Sequence comparison of *K. kingae* PilC1 with *P. aeruginosa* PilY1 highlighting the C-terminal region with the greatest amount of homology (in black). Sequence identity and similarity values are given for the region in black. White bars represent putative and confirmed calcium-binding domains in *K. kingae* and *P. aeruginosa*, respectively. (B) Alignment of the *K. kingae* PilC1 putative Ca-binding site with the calcium-chelating residues of *P. aeruginosa* PilY1, with the potential calcium-chelating residues of PilC1 shown in bold. (C) Sequence comparison of *K. kingae* PilC2 with *P. aeruginosa* PilY1 highlighting the C-terminal region with the greatest amount of homology (in black). Sequence identity and similarity values are given for the region in black. White bars represent putative and confirmed calcium-binding domains in *K. kingae* and *P. aeruginosa*, respectively. The white bar with an asterisk in the *K. kingae* PilC2 sequence represents a site homologous to a CaM calcium-binding site that does not bind calcium. (D) Alignment of the *K. kingae* PilC2 putative Ca-binding sites, with the calcium-chelating residues of human calmodulin and the potential calcium-chelating residues of PilC2 shown in bold.

$PilC1_{739-1047}$D930A-MBP and $PilC1_{739-1047}$D930K-MBP exhibited wild-type CD spectra (see Fig. S1 in the supplemental material), indicating that the overall structure of these fusion proteins was not altered.

In order to characterize PilC2, a recombinant fragment containing amino acids 868 to 1502 was purified. As shown in Fig. 2B, purified $PilC2_{868-1502}$ exhibited a binding affinity for calcium with a K_d of 5.5 μM, confirming that PilC2 binds calcium. This K_d is consistent with the previously published calmodulin values in the low micromolar range (37). Mutation of the terminal bidentate aspartic acid residue D1444 in the PilC2 Ca-binding loop to alanine or lysine eliminated Ca binding. The $PilC2_{868-1502}$D1444A and $PilC2_{868-1502}$D1444K proteins exhibited WT CD spectra and melting temperatures (see Fig. S2 in the supplemental material), indicating that the overall structure of these proteins was not altered. The less conserved 12-amino-acid site located at positions 1114 to 1125 was demonstrated to have no effect on Ca binding (Fig. 2C).

Taken together, these data indicate that PilC1 contains a functional Ca-binding site located in the region corresponding to amino acids 922 to 930 and that PilC2 contains a functional Ca-binding site located in the region corresponding to amino acids 1433 to 1444.

Influence of *K. kingae* PilC1 and PilC2 Ca-binding sites on type IV pilus production. To investigate the influence on and role of the PilC1 and PilC2 Ca-binding sites in type IV pilus production and other type IV pilus phenotypes in *K. kingae*, we generated a series of mutants in the KK03 strain background, a naturally occurring spreading and corroding derivative of 269-492 that produces stable levels of type IV pili. The *pilC1* and *pilC2* genes are located in physically separate regions of the *K. kingae* genome, as highlighted in the diagrams of the mutant derivatives of KK03 in Fig. 3. To investigate the phenotypes associated with an individual *pilC* locus, Ca-binding site mutations were introduced into the *pilC* locus of interest with a nearby antibiotic resistance marker in a strain background with the other *pilC* gene deleted. Strains containing Ca-binding mutations in both PilC1 and PilC2 were also generated for investigation. In addition to the strains diagrammed in Fig. 3, a previously described Δ*pilF* type IV pilus assembly ATPase mutant that is unable to assemble type IV pili was used as a control strain (14).

To assess production of type IV pili, fibers were sheared from the surfaces of equal-OD_{600} suspensions of *K. kingae* KK03 derivatives and separated using SDS-PAGE, and the major pilin subunit was stained with Coomassie blue. In earlier work, we demonstrated that the major band at ~14 kDa is PilA1, the major pilin subunit (15). As shown in Fig. 4, while the Δ*pilF* and Δ*pilC1* Δ*pilC2* strains were nonpiliated, all mutants that produced at least one PilC protein (whether WT or containing a mutation in the Ca-binding site) were piliated. The type IV pilus retraction machinery mutant Δ*pilT* was included as a control and was piliated (38). In some strains, there appeared to be slight reductions in quantity of extracellular PilA1 relative to the parental strains, including Δ*pilC2* PilC1D930A, Δ*pilC2* PilC1D930K, and PilC1D930A PilC2D1444A strains, indicating a minor defect in surface pilus production (Fig. 4). However, all strains examined produced surface pili, demonstrating that Ca-binding site mutant PilC1 and PilC2 are still able to promote piliation. Examination of this strain set using TEM revealed no noticeable changes in pilus number per bacterium and no differences in pilus length or morphology (data not shown). Together, these data indicate that at least one PilC protein is required to promote piliation and that the Ca-binding sites are dispensable for piliation.

The PilC1 and PilC2 Ca-binding sites influence twitching motility. We next wanted to assess the role of the PilC Ca-binding sites in twitching motility. Using a modified agar plate stab assay originally developed for use in *P. aeruginosa* (35), we measured the spreading zone at the plate-agar interface as a readout for twitching motility. We demonstrated the utility of this method for assessing twitching motility by showing that a strain lacking PilT, the type IV pilus retraction ATPase, still produced surface pili but was unable to form a spreading zone (38). As shown in Fig. 5, the Δ*pilC2* and control Δ*pilC2* PilC1mark strains produced statistically significantly larger twitching zones than did the parent strain ($P < 0.05$), while the Δ*pilC1* and Δ*pilC1* PilC2mark strains produced twitching zones that were slightly smaller than but were not statistically significantly different from those of the parent strain. These data indicate that PilC1 and PilC2 differentially control twitching motility and that PilC2 serves to dampen twitching motility when PilC1 is present. Interestingly, the PilC1D930A and PilC1D930K mutations exhibited significantly reduced twitching motility compared to the parent and wild-type strains ($P < 0.05$), similar to the nontwitching
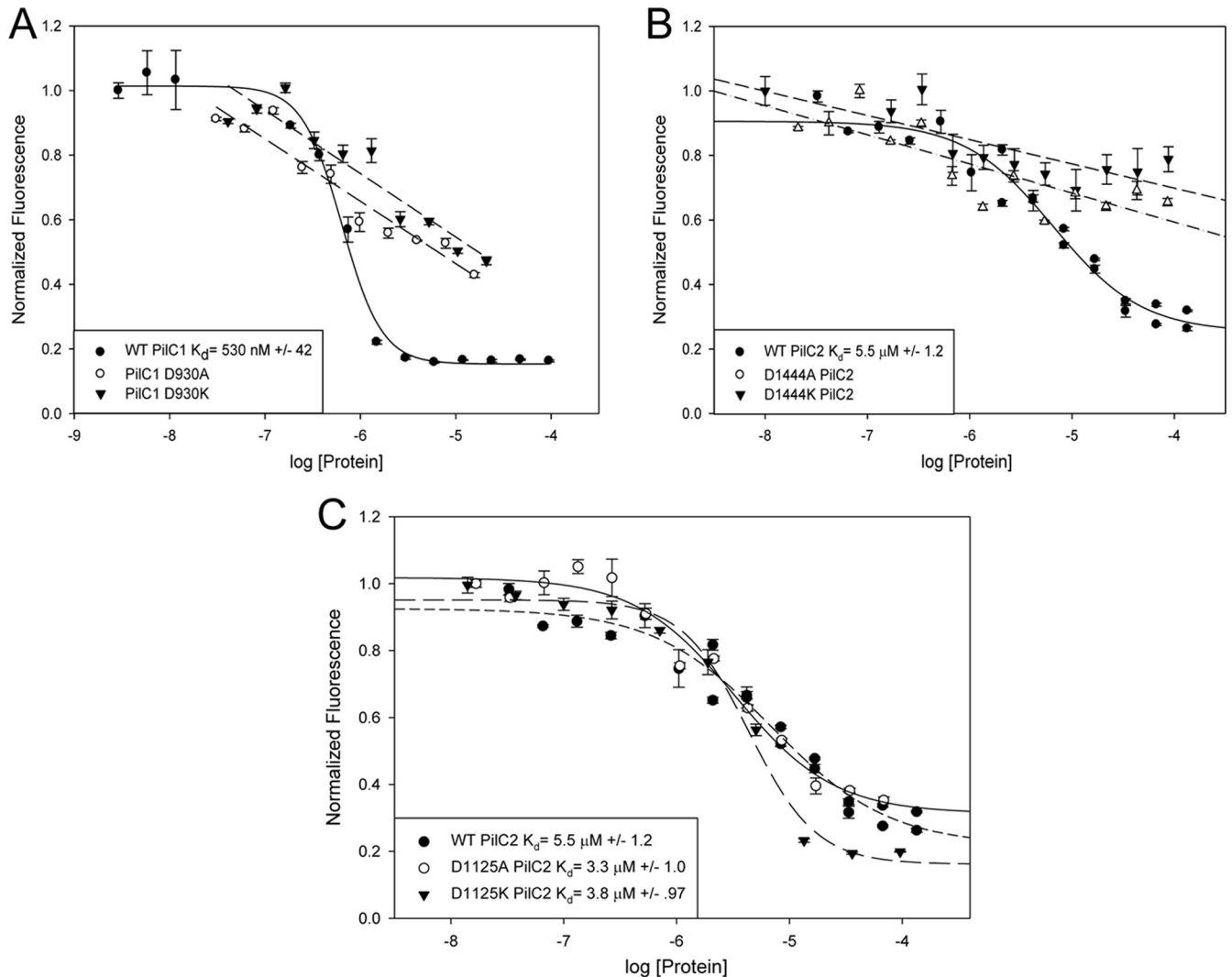
FIG 2 *K. kingae* PilC1 and PilC2 contain calcium-binding sites. Calcium competition binding assays using Oregon green were performed with WT, D930A, and D930K recombinant PilC1$_{739-1047}$-MBP (A); WT, D1444A, and D1444K recombinant PilC2$_{868-1502}$ (B); and WT, D1125A, and D1125 recombinant PilC2$_{868-1502}$ (C). Binding curves were modeled to one-site competition or linear line. Error bars represent standard errors of the means.

Δ*pilF* and Δ*pilC1* Δ*pilC2* strains. In contrast, the Δ*pilC1* PilC2D1444A strain demonstrated no defect in twitching motility compared to the parental Δ*pilC1* strain and control Δ*pilC1* PilC2mark strain, while the Δ*pilC1* PilC2D1444K strain had a modest but statistically significant ($P < 0.05$) reduction in twitching zone. Reduced twitching zones were also evident for the PilC1D930A PilC2D1444A and PilC1D930K PilC2D1444K double mutants compared to those of the parental and wild-type strains. Despite the smaller twitching zones in these three mutants, the zones were significantly larger than the zones produced by the twitching-deficient controls ($P < 0.05$), indicating reduced and not absent twitching motility. Compared to the wild-type strain, the mutants fall into four distinct statistically significant categories: null (Δ*pilF*, Δ*pilC1* Δ*pilC2*, Δ*pilC2* PilC1D930A, and Δ*pilC2* PilC1D930K strains), WT (WT, Δ*pilC1*, Δ*pilC1* PilC2mark, and Δ*pilC1* PilC2D1444A strains), <WT (Δ*pilC1* PilC2D1444K, PilC1D930A PilC2D1444A, and PilC1D930K PilC2D1444K strains), and >WT (Δ*pilC2* and Δ*pilC2* PilC1mark strains). Together, these

data demonstrate that the PilC1 Ca-binding site is essential for twitching motility, while the PilC2 Ca-binding site has only a minor influence on twitching motility.

The PilC1 Ca-binding site but not the PilC2 Ca-binding site is necessary for adherence. We next chose to investigate the influence of PilC1 and PilC2 Ca binding on adherence to human epithelial cells. Using a previously established adherence assay (14, 15), we determined the relative levels of adherence to Chang epithelial cells by the series of Ca-binding site mutants. Of note, we previously observed reduced adherence of the 269-492Δ*pilC1* and 269-492*pilC2::aphA3* mutants compared to strain 269-492 (14). In contrast, in this study, the Δ*pilC1* derivative of KK03 had only a slight defect in adherence, and the Δ*pilC2* derivative of KK03 had no defect in adherence, compared to the KK03 parent (Fig. 6). Examination of the adherence to Chang cells by the PilC Ca-binding mutants revealed stark differences between PilC1 and PilC2 (Fig. 6). The Δ*pilC2* PilC1D930A and Δ*pilC2* PilC1D930K strains exhibited marked deficiencies in adherence compared to the
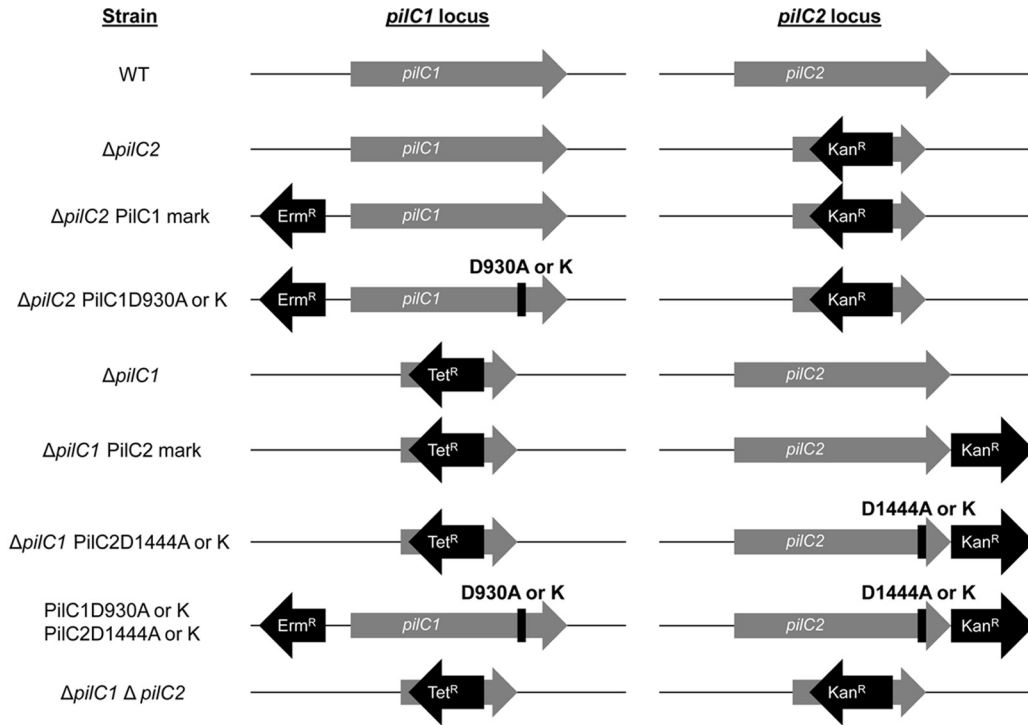
FIG 3 Representation of the *pilC1* and *pilC2* loci of *K. kingae* strain KK03 derivatives used in this study. The *pilC1* and *pilC2* genes are present at separate loci in the genome. The Δ*pilC1* and Δ*pilC2* mutants are marked with a tetracycline resistance cassette (Tet[r]) and a kanamycin resistance cassette (Kan[r]), respectively. Both deletion mutations were combined to generate the Δ*pilC1* Δ*pilC2* double mutant. Δ*pilC2* PilC1D930A and Δ*pilC2* PilC1D930K strains, with a Δ*pilC2* PilC1mark strain (WT *pilC1* with an erythromycin resistance cassette [Erm[r]] upstream of the promoter region) used as a control, were generated to study the role of the PilC1 Ca-binding site in the absence of *pilC2*. Δ*pilC1* PilC2D1444A and Δ*pilC1* PilC2D1444K strains, with a Δ*pilC1* PilC2mark strain (WT *pilC2* with the Kan[r] marker immediately downstream of *pilC2*) used as a control, were generated to study the role of the PilC2 Ca-binding site in the absence of *pilC1*. Mutations were combined to generate PilC1D930A PilC2D1444A and PilC1D930K PilC2D1444K strains.

Δ*pilC2* and Δ*pilC2* PilC1mark control strains ($P < 0.05$) and ad- hered at levels similar to those of the nonpiliated Δ*pilF* and Δ*pilC1* Δ*pilC2* controls. However, the Δ*pilC1* PilC2D1444A and Δ*pilC1* PilC2D1444K strains displayed normal adherence, comparable to adherence by the parental Δ*pilC1* and Δ*pilC1* PilC2mark control strains. The PilC1D930A PilC2D1444A and PilC1D930K PilC2D1444K double mutants also adhered at levels similar to those of the Δ*pilC1* strains that express either WT or mutant PilC2, indicating that PilC2 is able to promote adherence in the presence of Ca-binding mutant PilC1, regardless of PilC2 Ca-binding state. These results demonstrate that the PilC1 Ca-bind-ing site is necessary and the PilC2 Ca-binding site is dispensable for adherence to Chang cells.
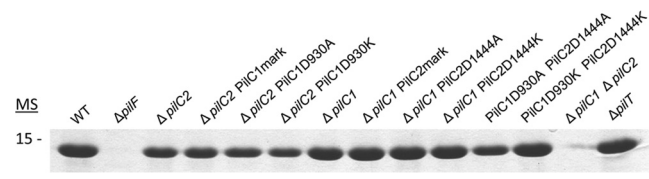
FIG 4 All PilC1 and PilC2 Ca-binding-site mutants produce surface pili. Pili were sheared from the surface of *K. kingae* strain KK03 derivatives, and the major pilin subunit, PilA1, was visualized with Coomassie blue staining fol-lowing SDS-PAGE. Δ*pilF* and Δ*pilC1* Δ*pilC2* strains both express PilA1 but fail to assemble surface pili, and the Δ*pilT* strain is a pilus retraction mutant and is piliated. MS, molecular size (in kDa).
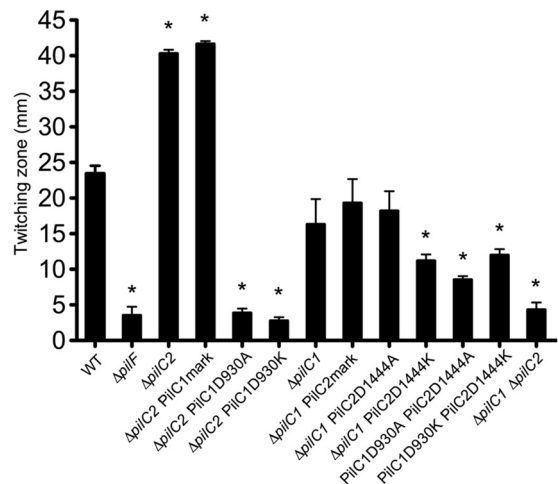
FIG 5 The PilC1 and PilC2 Ca-binding sites influence twitching motility. *K. kingae* strain KK03 and derivatives were assessed for twitching motility using a modified agar plate stab assay. Twitching-zone diameters were measured in triplicate, and averages were calculated from three independent experiments. Error bars represent standard errors of the means. Statistical analysis was per-formed using ANOVA with Bonferroni's posttest to compare twitching-mo-tility zones between the mutants and the parental strains as noted in the text. Asterisks indicate statistically significant ($P < 0.05$) differences between the mutants and the relevant parental strain.
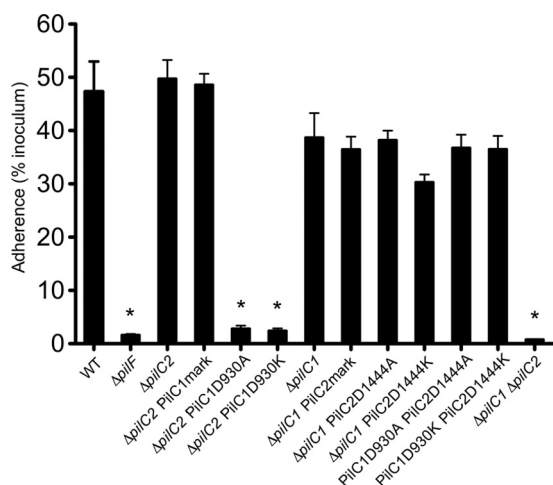
FIG 6 The PilC1 but not PilC2 Ca-binding site is essential for adherence. *K. kingae* strain KK03 and derivatives were investigated for adherence to Chang human epithelial cells using a quantitative adherence assay. Experiments were performed in triplicate, and averages were calculated from three independent experiments. Error bars represent standard errors of the means. Statistical analysis was performed using ANOVA and Bonferroni's posttest to compare adherence levels between the mutants and the parental strains as noted in the text. Asterisks indicate statistically significant ($P < 0.05$) differences between the mutants and the relevant parental strain.

DISCUSSION

K. kingae produces type IV pili that mediate adherence to human cells (14, 15). The PilC-like proteins play key roles in type IV pilus biology in *K. kingae* and numerous other Gram-negative bacteria of medical importance (17, 18). In this study, we found that PilC1 and PilC2 bind calcium *in vitro* and that significant differences in type IV pilus phenotypes exist in the PilC1 and PilC2 Ca-binding-site mutants. Both wild-type and Ca-binding mutant PilC1 and PilC2 were able to promote pilus production when expressed individually. However, Ca-binding mutant PilC1 eliminated twitching motility and adherence, while Ca-binding mutant PilC2 had little or no effect on twitching motility and no effect on adherence. Strains that expressed both PilC1 and PilC2 Ca-binding mutants demonstrated phenotypes identical to those of the PilC2 single mutant. These data demonstrate important differences in PilC1 and PilC2 control of type IV pilus phenotypes in *K. kingae*.

In the pathogenic *Neisseria* species, PilC1 and PilC2 are highly homologous to each other. *N. gonorrhoeae* PilC1 and PilC2 function interchangeably in promoting pilus biogenesis, natural competence, and adherence (39, 40). *N. meningitidis* PilC1 and PilC2 both promote pilus production and natural competence but differentially promote adherence to certain cell types (28, 30, 41, 42). Sequence analysis suggests that differences in PilC1- and PilC2-mediated adherence are based in the N-terminal portion of the proteins (43). Given the highly homologous nature of the PilC proteins in the pathogenic *Neisseria* species, especially in the C-terminal portion of the protein and in the 9-amino-acid putative Ca-binding loop, it is likely that Ca binding is an important factor for *Neisseria* type IV pilus biology. In contrast, the related *Neisseriaceae* family member *K. kingae* expresses two PilCs that share only limited sequence homology and are differentially controlled by Ca binding. We speculate that differences in host niches may be a driving factor influencing the mechanism of PilC function. *K.*

kingae inhabits the posterior pharynx as a commensal but tends to cause disease primarily in the joints and bones, two calcium-rich sites. Of note, human plasma has a free calcium concentration of 1.03 to 1.30 mM, and human joint fluid has a calcium concentration of 4 mM or higher (44). These high-calcium environments may promote the Ca-dependent functions of PilC1, with no specific effect on PilC2. While calcium is the predominant divalent cation associated with the 9-amino-acid and 12-amino-acid consensus binding motifs, magnesium, zinc, and manganese may bind to these motifs as well (32, 45–48). In future studies, we will examine whether these additional divalent cations influence PilC1 or PilC2 function.

The first report that calcium plays a key role in regulating type IV pilus production and twitching motility described the study of PilY1, a PilC-like protein in *P. aeruginosa* (34). Orans et al. crystallized the C-terminal domain of PilY1 and identified a 9-amino-acid Ca-binding site. These investigators showed that mutation of the bidentate aspartic acid residue in the Ca-binding loop to alanine (D859A) resulted in significantly reduced pilus production and twitching motility, mimicking the effect of a Δ*pilY1* mutation. Mutation of the same residue to lysine resulted in increased pilus production and reduced twitching motility, mimicking a Δ*pilT* pilus retraction mutation. Interestingly, *K. kingae* PilC1 contains a similar 9-amino-acid site, and mutation of the predicted bidentate residue to alanine or lysine eliminated twitching motility but did not have a major impact on surface pilus production, thus contrasting with PilY1. Hence, while control of twitching motility in PilY1 is due to the influence of the Ca-binding site on pilus production, the *K. kingae* PilC1 Ca-binding site directly impacts twitching motility and adherence, not surface pilus production. Interestingly, expression of the alanine or lysine mutant proteins in *K. kingae* resulted in identical phenotypes, again contrasting with PilY1. Orans et al. modeled the PilY1 D859K mutation and found that the amino group of the lysine side chain potentially mimics a calcium ion, creating a pseudo-calcium-bound PilY1 state. One potential reason for the differences observed between the *K. kingae* PilC1D930K mutant and the PilY1D859K mutant may be differences in the structures of the regions surrounding the Ca-binding loop in the two proteins, as the primary amino acid sequence of the loop is largely conserved (Fig. 1B).

To dissect the roles of PilC1 and the Ca-binding site in *K. kingae* type IV pilus-mediated twitching motility and adherence, it is important to examine the relationship between the two phenotypes. We have found that disruption of the *K. kingae* type IV pilus retraction machinery, *pilTU*, results in increased surface piliation, significantly reduced adherence, and loss of twitching motility (38). Interestingly, adherence by the Δ*pilT* mutant is reduced to approximately 50% of the wild type (38) rather than eliminated, as observed with the Δ*pilC2* PilC1D930A and Δ*pilC2* PilC1D930K mutants (Fig. 6). Taken together, these data suggest that the adherence defect of these two mutants is not completely a result of the defect in twitching motility but is a consequence of altered PilC1 adherence-promoting activity. In accord with these findings, Johnson et al. found that *in vitro* Ca binding by *P. aeruginosa* PilY1 influences RGD-mediated PilY1 binding to integrins, supporting a specific role for the 9-amino-acid Ca-binding site in adherence in this protein class (32).

In contrast to the situation with PilC1, the *K. kingae* PilC2 Ca-binding site is dispensable for twitching motility and adherence. We originally identified two potential Ca-binding sites in

PilC2 with homology to the 12-amino-acid Ca-binding loop of human calmodulin and no sites with homology to the PilY1-like loop. *In vitro* analysis demonstrated that only one of these sites was functional. However, our data clearly show that PilC2 is able to promote pilus production, twitching motility, and adherence when the confirmed Ca-binding site is mutated. These results suggest that *K. kingae* PilC1 and PilC2 utilize different mechanisms in relation to Ca binding to promote twitching motility and adherence.

At this time, we can only speculate on the potential mechanisms by which Ca binding by PilC1 and PilC2 influences type IV pilus phenotypes. In the case of PilC1, we suggest that Ca binding or Ca responsiveness may be essential for proper protein structure. In this model, the Ca-binding-site mutant PilC1 has an altered protein conformation that retains the ability to promote pilus assembly but is not able to promote twitching motility and adherence. In contrast, PilC2 appears to function completely independently of Ca binding at the site identified in this report (Fig. 1B). We envision two potential scenarios to explain our findings: (i) PilC2 contains an additional cryptic Ca-binding site in the N-terminal 857 amino acids that were not included in the PilC2 fragment used for the *in vitro* Ca-binding studies, or (ii) PilC2 utilizes a novel mechanism that promotes twitching motility and adherence regardless of the functionality of the Ca-binding site. In the study by Johnson et al. that identified RGD-mediated PilY1 binding to integrins, analysis revealed a second Ca-binding site in PilY1 (32). While sequence analysis of PilC2 did not reveal any additional potential Ca-binding sites, we cannot rule out this possibility.

The results presented in this report establish key differences in the role of Ca binding in the function of the *K. kingae* PilC1 and PilC2 proteins. However, the precise mechanisms used by these proteins to control type IV pilus phenotypes remain unclear and will require future investigation. A greater understanding of *K. kingae* PilC1 and PilC2 function may provide insights into species-specific control mechanisms of type IV pilus phenotypes and suggest novel strategies for prevention or treatment of *K. kingae* disease.

REFERENCES

1. **Chometon S, Benito Y, Chaker M, Boisset S, Ploton C, Berard J, Vandenesch F, Freydiere AM.** 2007. Specific real-time polymerase chain reaction places *Kingella kingae* as the most common cause of osteoarticular infections in young children. Pediatr. Infect. Dis. J. **26**:377–381.

2. **Gené A, Garcia-Garcia JJ, Sala P, Sierra M, Huguet R.** 2004. Enhanced culture detection of *Kingella kingae*, a pathogen of increasing clinical importance in pediatrics. Pediatr. Infect. Dis. J. **23**:886–888.

3. **Lehours P, Freydiere AM, Richer O, Burucoa C, Boisset S, Lanotte P, Prere MF, Ferroni A, Lafuente C, Vandenesch F, Megraud F, Menard A.** 2011. The *rtxA* toxin gene of *Kingella kingae*: a pertinent target for molecular diagnosis of osteoarticular infections. J. Clin. Microbiol. **49**:1245–1250.

4. **Moumile K, Merckx J, Glorion C, Berche P, Ferroni A.** 2003. Osteoarticular infections caused by *Kingella kingae* in children: contribution of polymerase chain reaction to the microbiologic diagnosis. Pediatr. Infect. Dis. J. **22**:837–839.

5. **Verdier I, Gayet-Ageron A, Ploton C, Taylor P, Benito Y, Freydiere AM, Chotel F, Berard J, Vanhems P, Vandenesch F.** 2005. Contribution of a broad range polymerase chain reaction to the diagnosis of osteoarticular infections caused by *Kingella kingae*: description of twenty-four recent pediatric diagnoses. Pediatr. Infect. Dis. J. **24**:692–696.

6. **Yagupsky P.** 2004. *Kingella kingae*: from medical rarity to an emerging paediatric pathogen. Lancet Infect. Dis. **4**:358–367.

7. **Yagupsky P, Dagan R, Howard CW, Einhorn M, Kassis I, Simu A.** 1992.

8. **Yagupsky P, Porsch E, St Geme JW, III.** 2011. *Kingella kingae*: an emerging pathogen in young children. Pediatrics **127**:557–565.

9. **Yagupsky P, Dagan R, Prajgrod F, Merires M.** 1995. Respiratory carriage of *Kingella kingae* among healthy children. Pediatr. Infect. Dis. J. **14**:673–678.

10. **Yagupsky P, Peled N, Katz O.** 2002. Epidemiological features of invasive *Kingella kingae* infections and respiratory carriage of the organism. J. Clin. Microbiol. **40**:4180–4184.

11. **Yagupsky P, Porat N, Pinco E.** 2009. Pharyngeal colonization by *Kingella kingae* in children with invasive disease. Pediatr. Infect. Dis. J. **28**:155–157.

12. **Yagupsky P, Weiss-Salz I, Fluss R, Freedman L, Peled N, Trefler R, Porat N, Dagan R.** 2009. Dissemination of *Kingella kingae* in the community and long-term persistence of invasive clones. Pediatr. Infect. Dis. J. **28**:707–710.

13. **Basmaci R, Ilharreborde B, Bidet P, Doit C, Lorrot M, Mazda K, Bingen E, Bonacorsi S.** 2012. Isolation of *Kingella kingae* in the oropharynx during *K. kingae* arthritis in children. Clin. Microbiol. Infect. **18**:E134–E136. doi:10.1111/j.1469-0691.2012.3799.x.

14. **Kehl-Fie TE, Miller SE, St Geme JW, III.** 2008. *Kingella kingae* expresses type IV pili that mediate adherence to respiratory epithelial and synovial cells. J. Bacteriol. **190**:7157–7163.

15. **Kehl-Fie TE, Porsch EA, Miller SE, St Geme JW, III.** 2009. Expression of *Kingella kingae* type IV pili is regulated by sigma54, PilS, and PilR. J. Bacteriol. **191**:4976–4986.

16. **Kehl-Fie TE, Porsch EA, Yagupsky P, Grass EA, Obert C, Benjamin DK, Jr, St Geme JW, III.** 2010. Examination of type IV pilus expression and pilus-associated phenotypes in *Kingella kingae* clinical isolates. Infect. Immun. **78**:1692–1699.

17. **Pelicic V.** 2008. Type IV pili: e pluribus unum? Mol. Microbiol. **68**:827–837.

18. **Burrows LL.** 2005. Weapons of mass retraction. Mol. Microbiol. **57**:878–888.

19. **Wolfgang M, Lauer P, Park HS, Brossay L, Hebert J, Koomey M.** 1998. PilT mutations lead to simultaneous defects in competence for natural transformation and twitching motility in piliated *Neisseria gonorrhoeae*. Mol. Microbiol. **29**:321–330.

20. **Anantha RP, Stone KD, Donnenberg MS.** 1998. Role of BfpF, a member of the PilT family of putative nucleotide-binding proteins, in type IV pilus biogenesis and in interactions between enteropathogenic *Escherichia coli* and host cells. Infect. Immun. **66**:122–131.

21. **Chiang P, Sampaleanu LM, Ayers M, Pahuta M, Howell PL, Burrows LL.** 2008. Functional role of conserved residues in the characteristic secretion NTPase motifs of the *Pseudomonas aeruginosa* type IV pilus motor proteins PilB, PilT and PilU. Microbiology **154**:114–126.

22. **Merz AJ, So M, Sheetz MP.** 2000. Pilus retraction powers bacterial twitching motility. Nature **407**:98–102.

23. **Whitchurch CB, Hobbs M, Livingston SP, Krishnapillai V, Mattick JS.** 1991. Characterisation of a *Pseudomonas aeruginosa* twitching motility gene and evidence for a specialised protein export system widespread in eubacteria. Gene **101**:33–44.

24. **Wolfgang M, Park HS, Hayes SF, van Putten JP, Koomey M.** 1998. Suppression of an absolute defect in type IV pilus biogenesis by loss-of-function mutations in pilT, a twitching motility gene in *Neisseria gonorrhoeae*. Proc. Natl. Acad. Sci. U. S. A. **95**:14973–14978.

25. **Heiniger RW, Winther-Larsen HC, Pickles RJ, Koomey M, Wolfgang MC.** 2010. Infection of human mucosal tissue by *Pseudomonas aeruginosa* requires sequential and mutually dependent virulence factors and a novel pilus-associated adhesin. Cell. Microbiol. **12**:1158–1173.

26. **Morand PC, Bille E, Morelle S, Eugene E, Beretti JL, Wolfgang M, Meyer TF, Koomey M, Nassif X.** 2004. Type IV pilus retraction in pathogenic *Neisseria* is regulated by the PilC proteins. EMBO J. **23**:2009–2017.

27. **Jonsson AB, Nyberg G, Normark S.** 1991. Phase variation of gonococcal pili by frameshift mutation in *pilC*, a novel gene for pilus assembly. EMBO J. **10**:477–488.

28. **Nassif X, Beretti JL, Lowy J, Stenberg P, O'Gaora P, Pfeifer J, Normark S, So M.** 1994. Roles of pilin and PilC in adhesion of *Neisseria meningitidis* to human epithelial and endothelial cells. Proc. Natl. Acad. Sci. U. S. A. **91**:3769–3773.

High prevalence of *Kingella kingae* in joint fluid from children with septic arthritis revealed by the BACTEC blood culture system. J. Clin. Microbiol. **30**:1278–1281.

29. **Rudel T, Scheurerpflug I, Meyer TF.** 1995. *Neisseria* PilC protein identified as type-4 pilus tip-located adhesin. Nature **373**:357–359.

30. **Rahman M, Kallstrom H, Normark S, Jonsson AB.** 1997. PilC of pathogenic *Neisseria* is associated with the bacterial cell surface. Mol. Microbiol. **25**:11–25.

31. **Scheuerpflug I, Rudel T, Ryll R, Pandit J, Meyer TF.** 1999. Roles of PilC and PilE proteins in pilus-mediated adherence of *Neisseria gonorrhoeae* and *Neisseria meningitidis* to human erythrocytes and endothelial and epithelial cells. Infect. Immun. **67**:834–843.

32. **Johnson MD, Garrett CK, Bond JE, Coggan KA, Wolfgang MC, Redinbo MR.** 2011. *Pseudomonas aeruginosa* PilY1 binds integrin in an RGD- and calcium-dependent manner. PLoS One **6**:e29629. doi:10.1371/journal.pone.0029629.

33. **Alm RA, Hallinan JP, Watson AA, Mattick JS.** 1996. Fimbrial biogenesis genes of *Pseudomonas aeruginosa*: *pilW* and *pilX* increase the similarity of type 4 fimbriae to the GSP protein-secretion systems and *pilY1* encodes a gonococcal PilC homologue. Mol. Microbiol. **22**:161–173.

34. **Orans J, Johnson MD, Coggan KA, Sperlazza JR, Heiniger RW, Wolfgang MC, Redinbo MR.** 2010. Crystal structure analysis reveals *Pseudomonas* PilY1 as an essential calcium-dependent regulator of bacterial surface motility. Proc. Natl. Acad. Sci. U. S. A. **107**:1065–1070.

35. **Alm RA, Mattick JS.** 1995. Identification of a gene, pilV, required for type 4 fimbrial biogenesis in *Pseudomonas aeruginosa*, whose product possesses a pre-pilin-like leader sequence. Mol. Microbiol. **16**:485–496.

36. **Kehl-Fie TE, St Geme JW, III.** 2007. Identification and characterization of an RTX toxin in the emerging pathogen *Kingella kingae*. J. Bacteriol. **189**:430–436.

37. **Linse S, Helmersson A, Forsen S.** 1991. Calcium binding to calmodulin and its globular domains. J. Biol. Chem. **266**:8050–8054.

38. **Porsch EA, Kehl-Fie TE, Geme JW, III.** 2012. Modulation of *Kingella kingae* adherence to human epithelial cells by type IV pili, capsule, and a novel trimeric autotransporter. mBio **3**:e00372-12. doi:10.1128/mBio.00372-12.

39. **Rudel T, van Putten JP, Gibbs CP, Haas R, Meyer TF.** 1992. Interaction of two variable proteins (PilE and PilC) required for pilus-mediated adherence of *Neisseria gonorrhoeae* to human epithelial cells. Mol. Microbiol. **6**:3439–3450.

40. **Rudel T, Facius D, Barten R, Scheuerpflug I, Nonnenmacher E, Meyer TF.** 1995. Role of pili and the phase-variable PilC protein in natural competence for transformation of *Neisseria gonorrhoeae*. Proc. Natl. Acad. Sci. U. S. A. **92**:7986–7990.

41. **Ryll RR, Rudel T, Scheuerpflug I, Barten R, Meyer TF.** 1997. PilC of *Neisseria meningitidis* is involved in class II pilus formation and restores pilus assembly, natural transformation competence and adherence to epithelial cells in PilC-deficient gonococci. Mol. Microbiol. **23**:879–892.

42. **Morand PC, Drab M, Rajalingam K, Nassif X, Meyer TF.** 2009. *Neisseria meningitidis* differentially controls host cell motility through PilC1 and PilC2 components of type IV pili. PLoS One **4**:e6834. doi:10.1371/journal.pone.0006834.

43. **Morand PC, Tattevin P, Eugene E, Beretti JL, Nassif X.** 2001. The adhesive property of the type IV pilus-associated component PilC1 of pathogenic *Neisseria* is supported by the conformational structure of the N-terminal part of the molecule. Mol. Microbiol. **40**:846–856.

44. **Maroudas A.** 1979. Physiochemical properties of articular cartilage, p 215–290. *In* Freeman MAR(ed), Adult articular cartilage. Pitman Medical, Kent, United Kingdom.

45. **Bogden JD, Singh NP, Joselow MM.** 1974. Cadmium, lead, and zinc concentrations in whole-blood samples of children. Environ. Sci. Technol. **8**:740–742.

46. **Kawasaki H, Kurosu Y, Kasai H, Isobe T, Okuyama T.** 1986. Limited digestion of calmodulin with trypsin in the presence or absence of various metal ions. J. Biochem. **99**:1409–1416.

47. **Milne DB, Sims RL, Ralston NV.** 1990. Manganese content of the cellular components of blood. Clin. Chem. **36**:450–452.

48. **Warren JT, Guo Q, Tang WJ.** 2007. A 1.3-A structure of zinc-bound N-terminal domain of calmodulin elucidates potential early ion-binding step. J. Mol. Biol. **374**:517–527.

49. **Sambrook J, Fritsch EF, Maniatis T.** 1989. Molecular cloning: a laboratory manual, 2nd ed. Cold Spring Harbor Laboratory Press, Cold Spring Harbor, NY.

50. **Stols L, Gu M, Dieckman L, Raffen R, Collart FR, Donnelly MI.** 2002. A new vector for high-throughput, ligation-independent cloning encoding a tobacco etch virus protease cleavage site. Protein Expr. Purif. **25**:8–15.

51. **Donnelly MI, Zhou M, Millard CS, Clancy S, Stols L, Eschenfeldt WH, Collart FR, Joachimiak A.** 2006. An expression vector tailored for large-scale, high-throughput purification of recombinant proteins. Protein Expr. Purif. **47**:446–454.

52. **Hendrixson DR, Akerley BJ, DiRita VJ.** 2001. Transposon mutagenesis of *Campylobacter jejuni* identifies a bipartite energy taxis system required for motility. Mol. Microbiol. **40**:214–224.

53. **Seifert HS.** 1997. Insertionally inactivated and inducible *recA* alleles for use in *Neisseria*. Gene **188**:215–220.

54. **Hamilton HL, Schwartz KJ, Dillard JP.** 2001. Insertion-duplication mutagenesis of *Neisseria*: use in characterization of DNA transfer genes in the gonococcal genetic island. J. Bacteriol. **183**:4718–4726.